

## POINTS OF SIGNIFICANCE

# The SEIRS model for infectious disease dynamics

Realistic models of epidemics account for latency, loss of immunity, births and deaths.

Ottar N. Bjørnstad, Katriona Shea, Martin Krzywinski and Naomi Altman

The simple but fundamental SIR framework introduced in the previous column<sup>1</sup> has been used to generate important insights about the evolution of a new epidemic in an idealized susceptible population with random mixing. Now we turn to how more complex disease transmission scenarios can be added to the model by introducing new compartments (groups) and more complicated flows between them. These will allow us to model important aspects such as birth, death, loss of immunity and age.

The basic SIR model<sup>1</sup> has three groups: susceptible (S), infectious (I) and recovered (R), with a total population size  $N = S + I + R$ . It is parametrized by the infectious period  $1/\gamma$ , the basic reproduction number  $R_0$  (the number of secondary cases for each infection in a completely susceptible population) and the contact rate  $\beta = \gamma R_0$ .

For most infectious diseases, however, there is a latent period between being infected and becoming infectious: the exposed group (E). Upon being infected, individuals will move to this group at a rate  $\beta SI/N$  and remain there for an average period of  $1/\sigma$  before moving into the I group. For many respiratory infections, immunity after recovery is temporary and recovered individuals will lose immunity and return to S after an average protected period of  $1/\omega$ .

Demography contributes to flows in and out of groups. Death due to infection will cause a loss of individuals from the I group at a rate  $\alpha$ , and all groups will experience background death from other causes at a rate  $\mu$ . In otherwise stable populations, background deaths are balanced by births into S at a rate  $\mu N$ .

Loss of immunity, births and deaths contribute to susceptible recruitment into S, which creates an 'open epidemic'. Ignoring vaccination<sup>1</sup>, these extensions (Fig. 1a) lead to the SEIRS model:

$$\begin{aligned}\frac{dS}{dt} &= \underbrace{\mu N}_{\text{birth}} - \underbrace{\beta SI/N}_{\text{infection}} + \underbrace{\omega R}_{\text{lost immunity}} - \underbrace{\mu S}_{\text{death}} \\ \frac{dE}{dt} &= \underbrace{\beta SI/N}_{\text{infection}} - \underbrace{\sigma E}_{\text{latency}} - \underbrace{\mu E}_{\text{death}}\end{aligned}$$

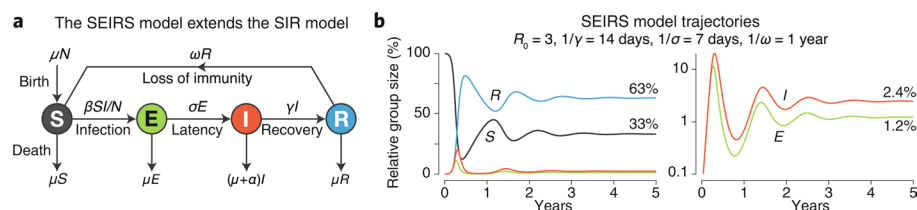


**Fig. 1 | The SEIRS model extends the SIR model and exhibits periodicity when  $R_0 > 1$  and there is recruitment into S. a**, The SEIRS model with demography. Rates are  $\beta$  (contact),  $\sigma$  (latency),  $\gamma$  (recovery),  $\omega$  (loss of immunity),  $\alpha$  (infection-induced death) and  $\mu$  (birth and background death). **b**, The SEIRS trajectory of S (black), E (green), I (orange) and R (blue) and their endemic equilibrium values for  $R_0 = 3$ ,  $1/\gamma = 14$  days,  $1/\sigma = 7$  days,  $1/\omega = 1$  year,  $1/\mu = 76$  years,  $\alpha = 0$  and  $\beta = 0.21/\text{day}$ . A closer view of the I and E trajectories is shown with log y axis. Calculations over 1,000 time steps with  $S(0) = 0.999$  and  $E(0) = 0.001$ ,  $I(0) = R(0) = 0$ .

$$\begin{aligned}\frac{dI}{dt} &= \underbrace{\sigma E}_{\text{latency}} - \underbrace{\gamma I}_{\text{recovery}} - \underbrace{(\mu + \alpha)I}_{\text{death}} \\ \frac{dR}{dt} &= \underbrace{\gamma I}_{\text{recovery}} - \underbrace{\omega R}_{\text{lost immunity}} - \underbrace{\mu R}_{\text{death}}\end{aligned}$$

The associated basic reproduction number is  $R_0 = [\sigma/(\sigma + \mu)] \times [\beta/(\sigma + \mu + \alpha)]$  because the infectious period is  $1/(\sigma + \mu + \alpha)$  and the probability of the index case becoming infectious rather than dying while in E is  $\sigma/(\sigma + \mu)$ . For most acute infections,  $\mu$  is much smaller than the epidemic rates so realistic values do not appreciably alter the trajectories (Fig. 2).

The trajectory of I lags that of E by the latency period, and (when  $R_0 > 1$ ) both E and I are predicted to eventually stabilize at an 'endemic equilibrium' that depends on all rates in the system<sup>2</sup> (Fig. 1b). For our scenario, this occurs after about 4 years, when the pathogen will circulate in the population with  $E = 1.2\%$  and  $I = 2.4\%$ , while  $S = 1/R_0 = 33\%$  (Fig. 1b).

In the presence of continuous susceptible recruitment, the path toward the endemic equilibrium will always occur in epidemic waves (Fig. 2). The inter-epidemic interval  $T_E$  is the wave period and is determined by rate parameters, host demography and pathogen characteristics<sup>2</sup>. These waves should not be confused with any seasonal cycles after the endemic equilibrium — the

latter result from seasonal variation in  $\beta$  (ref. <sup>3</sup>).

Increasing the latency period from  $1/\sigma = 7$  to 14 days increases the inter-epidemic interval from about  $T_E = 1.09$  to 1.29 years, but the waves attenuate at roughly the same rate and reach approximately the same equilibrium of  $I(\infty) = 2.4\%$  (Fig. 2a). If the period of immunity is doubled to  $1/\omega = 2$  years, the endemic equilibrium is halved to  $I(\infty) = 1.2\%$ , the inter-epidemic period is increased to  $T_E = 1.51$  years, and the time to settle on the equilibrium increases substantially because the mean SEIRS loop duration is longer (Fig. 2c).

A useful way to understand epidemic waves is with 'phase plane' plots that show the trajectory of I as a function of S (Fig. 2b,c). In this view, the waves trace out a spiral over time that converges to the endemic equilibrium, and this rate can be seen from the position of specific times on the spiral from the start of the first epidemic (for example, at the one-year mark, black points in Fig. 2b,c). For  $1/\sigma = 7$  days and  $1/\omega = 1$  year, the one-year mark on the trajectory (Fig. 2b, light orange) is just after the first trough in the wave. If we increase the latency period from  $1/\sigma = 7$  to 14 days, this point is closer to the trough (Fig. 2b, medium orange). The spiral is now traced out more slowly, reflecting the increase in the inter-epidemic interval  $T_E = 1.09$  to

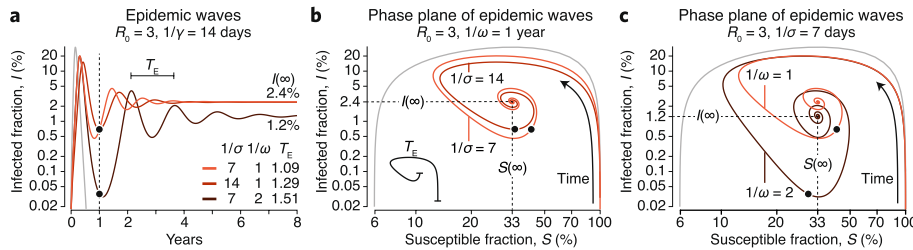


**Fig. 2 | The phenomenon of epidemic waves.** **a**, The trajectories of  $I$  for three different combinations of latency ( $1/\sigma$  days) and loss of immunity ( $1/\omega$  years) for  $R_0 = 3$ ,  $1/\gamma = 14$  days.  $T_E$  is the inter-epidemic interval (years),  $I(\infty)$  is the value at the endemic equilibrium and the gray trajectory is the prediction from the closed epidemic SIR model<sup>1</sup>. **b**, The  $I$  versus  $S$  phase planes of the  $1/\omega = 1$  year epidemic waves depicted in **a**, showing the effect of doubling  $1/\sigma$  from 7 to 14 days. **c**, The effect of doubling  $1/\omega$  from 1 to 2 years. Points along the spirals indicate the one-year mark after the start of the first epidemic. Start and progression of spirals are indicated by a black arrow (from bottom right and counterclockwise).

of the number of contacts ( $k$ ) and the probability of infection on contact ( $\pi$ )<sup>1</sup>. The severity of symptoms can affect  $\beta$  in various ways: a heavy cough that expels more infectious particles will increase  $\pi$ , whereas a debilitating illness that reduces contact will decrease  $k$ . This is relevant to the ongoing SARS-CoV-2 pandemic, in which the relationship between symptoms and infectiousness is not fully known. Such scenarios require that the  $I$  group be split into (for example) two or three with different groupings with respect to  $k$  and  $\pi$  (Fig. 3a).

Susceptible and infectious context may also be important. In the West African Ebola outbreak of 2013–2014, transmission in the community happened at a different rate than in hospitals<sup>3</sup>, with  $k$  and  $\pi$  both elevated for health care workers. Additionally, for hemorrhagic viruses like Ebola the possibility of post-mortem exposure during funeral preparations (group F) was an added risk factor (Fig. 3b). Age is also a critical determinant of severity for many infections, including SARS-CoV-2, and the basic compartmental framework can easily be extended to include contact patterns and transmission rates specific to age brackets (Fig. 3c).

Extensions such as those highlighted above are important when planning and prioritizing interventions. Next month we will discuss how to decide which model extensions are necessary in a given outbreak setting and how to use decision theory to identify the most critical knowledge gaps during an ongoing epidemic.

An interactive tool to explore the SEIRS model is at <https://martinkrz.github.io/posepi2>. □

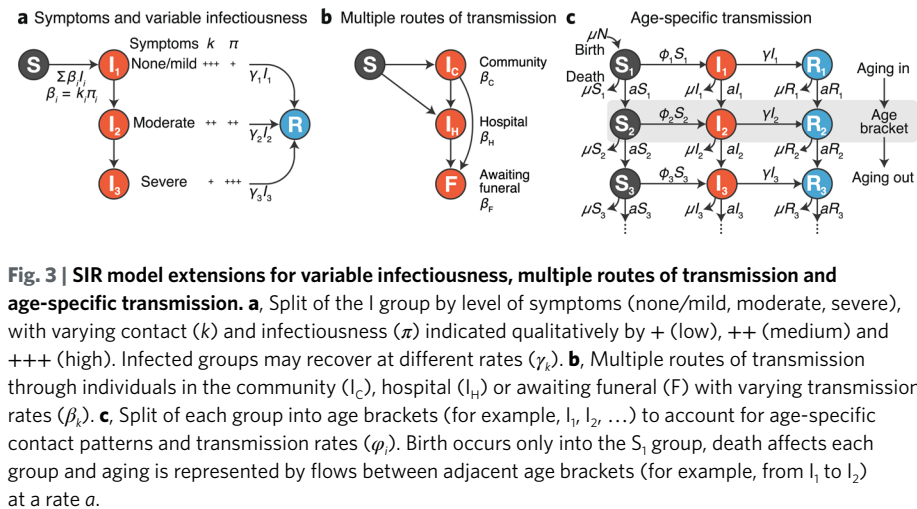


**Fig. 3 | SIR model extensions for variable infectiousness, multiple routes of transmission and age-specific transmission.** **a**, Split of the  $I$  group by level of symptoms (none/mild, moderate, severe), with varying contact ( $k$ ) and infectiousness ( $\pi$ ) indicated qualitatively by + (low), ++ (medium) and +++ (high). Infected groups may recover at different rates ( $\gamma_i$ ). **b**, Multiple routes of transmission through individuals in the community ( $I_c$ ), hospital ( $I_h$ ) or awaiting funeral ( $F$ ) with varying transmission rates ( $\beta_k$ ). **c**, Split of each group into age brackets (for example,  $I_1, I_2, \dots$ ) to account for age-specific contact patterns and transmission rates ( $\phi_i$ ). Birth occurs only into the  $S_1$  group, death affects each group and aging is represented by flows between adjacent age brackets (for example, from  $I_1$  to  $I_2$ ) at a rate  $a$ .

1.29 years, which in the phase plane is the time it takes for the spiral to complete a 360° loop (Fig. 2b, inset).

Doubling the duration of immunity from  $1/\omega = 1$  to 2 years leads to greater changes to the phase plane (Fig. 2c). Now the spiral center is shifted because the endemic equilibrium is halved to  $I(\infty) = 1.2\%$  and the spiral itself is stretched because of the greater fluctuation in  $I$  (and to a lesser extent in  $S$ ). The one-year mark is ahead of the first trough, reflecting a longer  $T_E = 1.51$  years.

The spiral paths of the open epidemic contrast to that of a ‘closed epidemic’ SIR model<sup>1</sup> with the same  $R_0$  and  $1/\gamma$  (Fig. 2, gray trace). The phase-plane SIR trajectory converges well before the one-year mark to  $I(\infty) = 0$  and a significantly smaller  $S(\infty)$  of 5.9%. In the case of an open epidemic,  $S(\infty) = 1/R_0$  is larger because of susceptible recruitment due to births and loss of immunity.

Neither the  $E$  nor  $I$  groups distinguish whether an individual has symptoms — only whether they are pre-infectious ( $E$ ) or infectious ( $I$ ). Typically,  $E$  will contain both asymptomatic and weakly symptomatic individuals who are not yet infectious, while the  $I$  group will mainly contain those who are symptomatic as well as any who are asymptomatic but nevertheless infectious. The  $R$  group may contain non-infectious symptomatic people, such as in the case of influenza, where symptoms commonly persist for several days after the virus has been cleared by the immune system.

Figure 3 illustrates how the SIR model can be extended to account for symptoms, multiple routes of transmission and age. For example, while symptoms and infectiousness often progress in parallel, they are not one and the same (Fig. 3a). Recall that the average rate at which an infected individual can infect a susceptible one ( $\beta$ ) is a product

Ottar N. Bjørnstad<sup>1,2</sup>, Katriona Shea<sup>1</sup>, Martin Krzywinski<sup>3</sup> and Naomi Altman<sup>4</sup>  
<sup>1</sup>Department of Biology, The Pennsylvania State University, State College, PA, USA. <sup>2</sup>Department of Entomology, The Pennsylvania State University, State College, PA, USA. <sup>3</sup>Canada’s Michael Smith Genome Sciences Centre, Vancouver, British Columbia, Canada. <sup>4</sup>Department of Statistics, The Pennsylvania State University, State College, PA, USA.  
 ✉e-mail: [martink@bcgsc.ca](mailto:martink@bcgsc.ca)

Published online: 4 June 2020  
<https://doi.org/10.1038/s41592-020-0856-2>

#### References

1. Bjørnstad, O. N., Shea, K., Krzywinski, M. & Altman, N. *Nat. Methods* **17**, 455–456 (2020).
2. Bjørnstad, O. N. *Epidemics: Models and Data Using R* (Springer, 2018).
3. Li, S.-L. et al. *Proc. Natl Acad. Sci. USA* **114**, 5659–5664 (2017).

#### Competing interests

The authors declare no competing interests.